



Synthesis, characterization and catalytic study of mesoporous carbon materials prepared via mesoporous silica using non-surfactant templating agents

Nitin S. Pagar^{1,3} · Prashant R. Karandikar² · Asha J. Chandwadkar² · Raj M. Deshpande¹

Accepted: 29 October 2020 / Published online: 9 November 2020
© Springer Science+Business Media, LLC, part of Springer Nature 2020

Abstract

Mesostructured silica materials with surface area in the range of ~700–900 m²/g have been prepared using hydroxy-carboxylic acid compounds such as tartaric acid, malic acid and citric acid (low cost non-surfactant template/pore forming agents) and tetraethylorthosilicate (TEOS) as silica source by sol-gel reaction. The templates were removed by either soxhlet extraction or calcination method. Mesoporous carbon molecular sieves were then prepared by carbonizing sucrose inside the pores of the above prepared mesoporous silica using sulfuric acid as a catalyst. The materials were characterized by FTIR spectroscopy, powder X-ray diffraction (XRD), N₂-sorption studies, microanalysis, thermal analysis and transmission electron microscopy (TEM). The resulting carbon material shows relatively higher surface area (~1100 m²/g), narrow pore size distribution and pore diameter of 4–5 nm. The mesoporosity of carbon material arises from interconnecting channels arrangements of mesoporous silica template. The mesoporous carbon material was used as a support for the immobilization of rhodium complex [HRhCO(TPPTS)₃] by ossification method. The prepared catalyst has been tested for the hydroformylation of higher olefins. The activity of the catalyst was improved by 20–30% as compared to the catalyst prepared from a conventional activated carbon support.

Keywords Low cost templates · Mesoporous silica · Carbonization · Mesoporous carbon · Immobilization · Hydroformylation

1 Introduction

The most important research area in the mesoporous materials is to develop an inexpensive and environmentally benign route for fabrication of three dimensionally interconnected mesoporous materials. Carbon with high surface

area, large pore volume and chemical inertness are useful in many material applications which includes adsorption, water and air purification, chromatographic column, capacitor for energy storage and as a catalyst support [1–6]. Most activated carbons synthesized through physical or chemical activation [7–11] are however microporous and these carbons have limited applications as adsorbents for large molecules and as an electrode [12, 13]. Various porous carbon materials have been fabricated using different kinds of nanostructural silica materials as templates. The technique consists of: (i) impregnation of the inorganic porous structure (template) with a carbon precursor (generally a polymer or prepolymer), (ii) carbonization of the precursor inside the nanocomposite, and (iii) elimination of the template that gives rise to the pores.

The recent discovery of ordered mesoporous materials thus provided a new generation to the silica templates [14–19]. These silica templates are suitable for the synthesis of mesoporous carbon, possibly with the ordered mesoporous structures with three dimensionally

Electronic supplementary material The online version of this article (<https://doi.org/10.1007/s10934-020-01003-x>) contains supplementary material, which is available to authorized users.

✉ Nitin S. Pagar
nitin.pagar@spcollegepune.ac.in; nspagar@gmail.com

¹ Homogeneous Catalysis Division, CSIR-National Chemical Laboratory, Dr. Homi Bhabha Road, Pune 411008, India

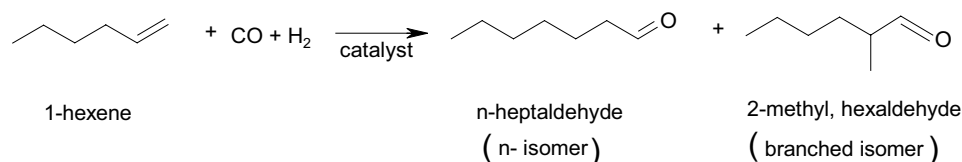
² Heterogeneous Catalysis Divisions, CSIR-National Chemical Laboratory, Dr. Homi Bhabha Road, Pune 411008, India

³ Post Graduate Department of Chemistry, Sir Parashurambhau College, Affiliated to Savitribai Phule Pune University, Pune 411030, India

interconnected channels. Ryoo and coworkers reported the first synthesis of new type of mesoscopically ordered carbon molecular sieve CMK-1 and CMK-3 (cubic and hexagonal respectively), by carbonizing sucrose inside the pores of the cubic MCM-48 and hexagonal SBA-15 mesostructured silica materials [20, 21]. Whereas furfuryl alcohol was found to be most suitable carbon precursor to synthesize hollow or fully filled cage-like silica-carbon mesostructures from SBA-16 [22]. Wormhole [23], foam like [24] mesostructured carbons and mesoporous

orthosilicate (TEOS) and using different concentrations of hydroxy-carboxylic acid as templates [33]. They have obtained mesoporous silica with numerous interconnected worm-like channels or pores which are relatively regular in diameter but largely disordered in channel arrangements.

The hydroformylation of olefins is one of the most important industrial processes exclusively relying on homogeneous catalysis [38]. This process produces the aldehydes by reaction of olefins with syngas in the presence of a catalyst as shown below:



carbons with high textural porosity [25] were fabricated using mesoporous aluminosilicate, organic colloids and mesostructured HMS silica materials as templates respectively. Kim and coworkers synthesized nanoporous hollow carbon tubes from silica tubes derived by sol-gel reactions of tetraethoxysilane and n-octadecyltrimethoxysilane on the surface of ammonium-dl tartarate crystals [26]. One-step synthesis of composite mesoporous carbon has also been reported on co-polymerization of cheap silica and carbon precursors [27].

The synthesis of mesoporous silica materials using surfactants as templates has been studied extensively [28–30]. So far surfactants, ionic [14, 17] or neutral [15, 31] have been the most commonly used templates for directing the formation of mesopores. All the ionic pathways are based on charge matching between the ionic surfactants and ionic inorganic precursors through electrostatic interactions. For the neutral surfactants it was suggested that hydrogen bonding between the surfactants and the precursors directs the formation of mesostructures. The preparation of mesoporous silica via neutral route has important advantage over electrostatic route because of the easy removal of the surfactants by solvent extraction and the tendency to produce material with thicker walls and smaller particle size. The second advantage is that they are relatively inexpensive, environmentally compatible and biodegradable.

Synthesis of mesoporous silica materials is documented in literature using the non-surfactant method [32–37]. A general non-surfactant neutral templating pathway for the preparation of mesoporous silica materials via sol-gel method with large surface area and pore volume is reported by Wei and coworkers, where he used D-glucose, D-maltose, dibenzoyl L-tartaric acid etc. as templates or pore forming agents [32]. Pang et al. reported the preparation of mesoporous silica materials via pre-hydrolysis of tetraethyl

Higher olefins (C_6 and onwards) constitutes more than 20% of the commercial hydroformylation capacity. Their hydroformylation is more complicated and has additional issues to that observed in lower olefin hydroformylation. (i) Isomerization of higher olefins under hydroformylation conditions is a prominent side reaction which ultimately affects the TON and n/i ratio. (ii) Heavy ends formation by side reactions such as condensation, trimerization, aldolization, acetalization at higher reaction temperatures. (iii) Catalyst-product separation is more difficult, as aldehydes of higher olefins are high boiling and their distillative separation from reaction mixture is difficult. Hence development of true heterogeneous catalyst for easy catalyst product separation is one of the challenging tasks in hydroformylation chemistry. Attempts were made to heterogenize the homogeneous catalysts by immobilization of the metal complex on a variety of organic/inorganic solid supports using different methods [39]. These methods includes anchoring [40, 41], tethering [42], encapsulation [43, 44], and impregnation of solid support with liquid medium containing catalyst i.e. supported liquid phase catalyst (SLPC) [45] and supported aqueous phase catalyst (SAPC) [46]. We have successfully demonstrated heterogenization of homogeneous complexes by the ossification method for carbonylation, hydroformylation and Suzuki cross coupling reactions [47–50].

Here, we report the synthesis of mesoporous silica at room temperature with short-range order and narrower pore size distribution by using hydroxy-carboxylic acids (tartaric, malic or citric acid) as templates/pore forming agents. Mesoporous carbon molecular sieves were then prepared by carbonizing sucrose inside the pores of the above prepared mesoporous silica using sulfuric acid. The above prepared mesoporous carbon is used as a support for preparation of immobilized rhodium complexes $[\text{HRhCO}(\text{TPPTS})_3]$ using ossification method in presence of excess trisodium salt of tris triphenyl

phosphine trisulphonate ligand (TPPTS) [48]. This catalyst has been found to be active for the hydroformylation of higher olefins such as 1-hexene, 1-octene and 1-decene.

2 Experimental

2.1 Chemicals

For the synthesis of mesoporous silica tetraethylorthosilicate (TEOS, Aldrich USA 98% pure), absolute ethanol (99.9%, S. D. Fine Chem. Ltd. India), hydrochloric acid (sp. gr. 1.18, 35.4%) tartaric acid, malic acid and citric acid (99% pure) purchased from Loba Chemie Pvt. Ltd. India. In order to prepare mesoporous carbon material sucrose (99.9% pure), H_2SO_4 (sp. gr. 1.8, 98% Pure), NaOH flakes (98% pure) were purchased from Loba Chemie Pvt. Ltd. India and used without further purification.

To prepare carbon supported barium salt of $\text{HRhCO}(\text{TPPTS})_3$ catalyst Rhodium trichloride ($\text{RhCl}_3 \cdot 3\text{H}_2\text{O}$, Arora-Matthey, India), Barium nitrate, PPh_3 , activated carbon (C-1) Loba Chemie Pvt. Ltd. India and used without further purification. The solvents, toluene, benzene, ethanol etc. were freshly distilled and dried prior to use. For hydroformylation experiments 1-hexene, 1-octene, 1-decene (>99% pure) procured from Aldrich USA. Hydrogen and nitrogen gas (Indian Oxygen, Mumbai, India), Carbon monoxide (>99.8% pure, Matheson Gas, USA) was used directly from the cylinders. The syngas mixture ($\text{H}_2 + \text{CO}$) with 1:1 ratio was prepared by mixing H_2 and CO in a reservoir vessel. The ligand triphenylphosphine trisulfonate (TPPTS) and its rhodium complex, $\text{HRh}(\text{CO})(\text{TPPTS})_3$ were prepared by known literature procedures [46, 51].

All the chemicals and reagents used were of analytical grade. Double distilled water was used during synthesis procedure.

2.2 Synthesis of mesoporous silica

Mesoporous silica was prepared on the basis of a procedure reported by Pang et al. with some modification [24]. The molar composition of the gel was: 1.0 [TEOS]: 0.01 [HCl]: 4.0 [H_2O]: 3.0 [EtOH]. Tetraethylorthosilicate (TEOS) in ethanol was hydrolyzed using hydrochloric acid as a catalyst in deionized water at room temperature in presence of an aqueous solution of hydroxy-carboxylic acid (0.45 g/ml for 50 wt%) as a template. The hydroxy-carboxylic acids used may be tartaric acid (T), malic acid (M) or citric acid (C) as template or pore forming agent. Slow hydrolysis in the presence of templates might play a role for some regularity in the mesophase formation.

The final gel was kept at room temperature for 1 month. The transparent monolithic disk obtained may be due to the aggregation/self-assembly formation of the template and their hydrogen bonding interactions with the inorganic precursor, which plays an important role in directing the mesostructure formation [14, 52]. This transparent, monolithic mesoporous silica disk containing template was then ground into fine powder and the template was removed by two methods: (a) soxhlet extraction using deionized water and (b) calcination at 550 °C (0.5 °C/min. in air) for 5–6 h. The soxhlet-extracted samples were designated as SSA (i.e., soxhlet extracted mesoporous silica of respective hydroxy-carboxylic acids). These are SST (tartaric acid templated silica), SSM (malic acid templated silica) and SSC (citric acid templated silica). For the calcined samples, the abbreviations are CSA (i.e. calcined mesoporous silica of respective hydroxy-carboxylic acids) i.e. CST, CSM and CSC as above respectively.

2.3 Synthesis of mesoporous carbon

In order to get the mesoporous carbon material, the mesoporous silica sample (prepared in Sect. 2.2) was impregnated with the aqueous solution of sucrose containing sulfuric acid, as reported earlier [20, 21]. In brief, 1 g of mesoporous silica material (SSA or CSA) was added to the solution obtained by dissolving 1 g of sucrose and 0.12 g of H_2SO_4 in 5 ml of H_2O . The mixture was placed in a drying oven for 6 h at 160 °C. The treatment was repeated and the obtained sample was carbonized under N_2 atmosphere at 900 °C (2 °C/min) for 5 h. The silica templates were then removed by dissolving in an ethanolic aqueous solution of sodium hydroxide. The mesoporous carbon samples thus produced were designated as SCA (carbon: using silica as template when procured on removing respective hydroxy-carboxylic acids by soxhlet extraction) and CCA (carbon: using silica as template when procured on removing respective hydroxy-carboxylic acids by calcination).

2.4 Preparation of carbon supported catalysts

The dispersed heterogenized catalyst was synthesized from a water-soluble metal complex prepared by known methods [51] and then supported ossified catalyst was prepared by precipitating it as its barium salt on a porous support as per the procedure described [48]. In a typical case, aqueous solution of 20% $\text{Ba}(\text{NO}_3)_2$ (0.060 g) was added to 0.3 g of carbon support. The mixture was refluxed for 4–5 h and evaporated to dryness to get barium nitrate impregnated carbon.

The carbon supported barium salt of $\text{HRhCO}(\text{TPPTS})_3$ was prepared by taking 0.3 g of above prepared $\text{Ba}(\text{NO}_3)_2$ impregnated carbon in a small two-neck round bottom flask.

An aqueous solution of $\text{HRhCO}(\text{TPPTS})_3$ [48 mg] and TPPTS [60 mg] was added under constant stirring in a positive flow of argon. The stirring was continued for 4–5 h. The mixture was filtered; the precipitate was washed 2–3 times with cold and hot water respectively followed by water and toluene for 12 h each with soxhlet apparatus, to remove the unreacted complex and excess ligand. The precipitate was dried under vacuum (yield=0.33 g.). Two catalysts thus prepared from activated carbon (C-1) and mesoporous carbons (SCT) were designated as Rh-C-1 and Rh-SCT respectively.

2.5 Characterization

FTIR spectra of mesoporous silica recorded with a Shimadzu FT-IR spectrometer (Model 8300). Mesoporous silica and carbon samples were characterized using X-ray diffraction method (Rigaku X-ray diffractometer; model Dmax 2500 with $\text{Cu K}\alpha$ radiations of $\lambda=0.154$ nm). The surface area and pore volume were determined from N_2 adsorption isotherms using a Coulter (Omnisorb, 100 CX) instrument. Metal content of the catalysts were analyzed by inductively coupled plasma with atomic emission spectra (ICP-AES) performed using Perkin-Elmer 1200 instrument. Transmission electron image was received from JEOL 1200 EX microscope operated at 100 kV. The sample was prepared by dispersing the powder in isopropanol. Depositing few drops of suspension on a carbon coated 400-mesh Cu grid enabled imaging. Thermal stability of the mesoporous silica/carbon samples was carried out using computer controlled thermal analyzer (Setaram, France, Model TG-DTA 92).

2.6 Catalytic experiment

The reactions were carried out in a 50 ml high-pressure stainless steel reactor manufactured by Amar Instruments, India. This reactor was fitted with a transducer for monitoring of pressure, a temperature control with automatic heating and cooling, and a magnetic stirrer with variable speed. A reservoir filled with syngas was connected to the reactor via a constant pressure regulator. This enabled continuous feeding of the syngas from the reservoir, as per the consumption in the reactor, while maintaining constant pressure in the reactor. The reaction was monitored by looking at the reservoir pressure drop. During the course of the reaction, the reactants and catalyst were charged into the reactor and the contents were flushed with nitrogen and syngas. Following this the reactor and contents were heated to the desired temperature under low stirring [200 rpm]. Once the temperature was attained, the syngas [$\text{CO}:\text{H}_2$, 1:1] were pressurized into the reactor as and when required. The reaction was started by increasing the agitation speed to 1400 rpm. The gas consumed by the reaction was made up by a continuous addition from the

reservoir, wherein the pressure was monitored with time. During the course of the reaction, samples were withdrawn periodically and analyzed on GC for reactant and products. At the end of the reaction the autoclave was cooled and final samples were taken for GC analysis (Agilent 6890, HP-5 capillary column 30 m) and confirmation of the mass balance.

3 Results and discussion

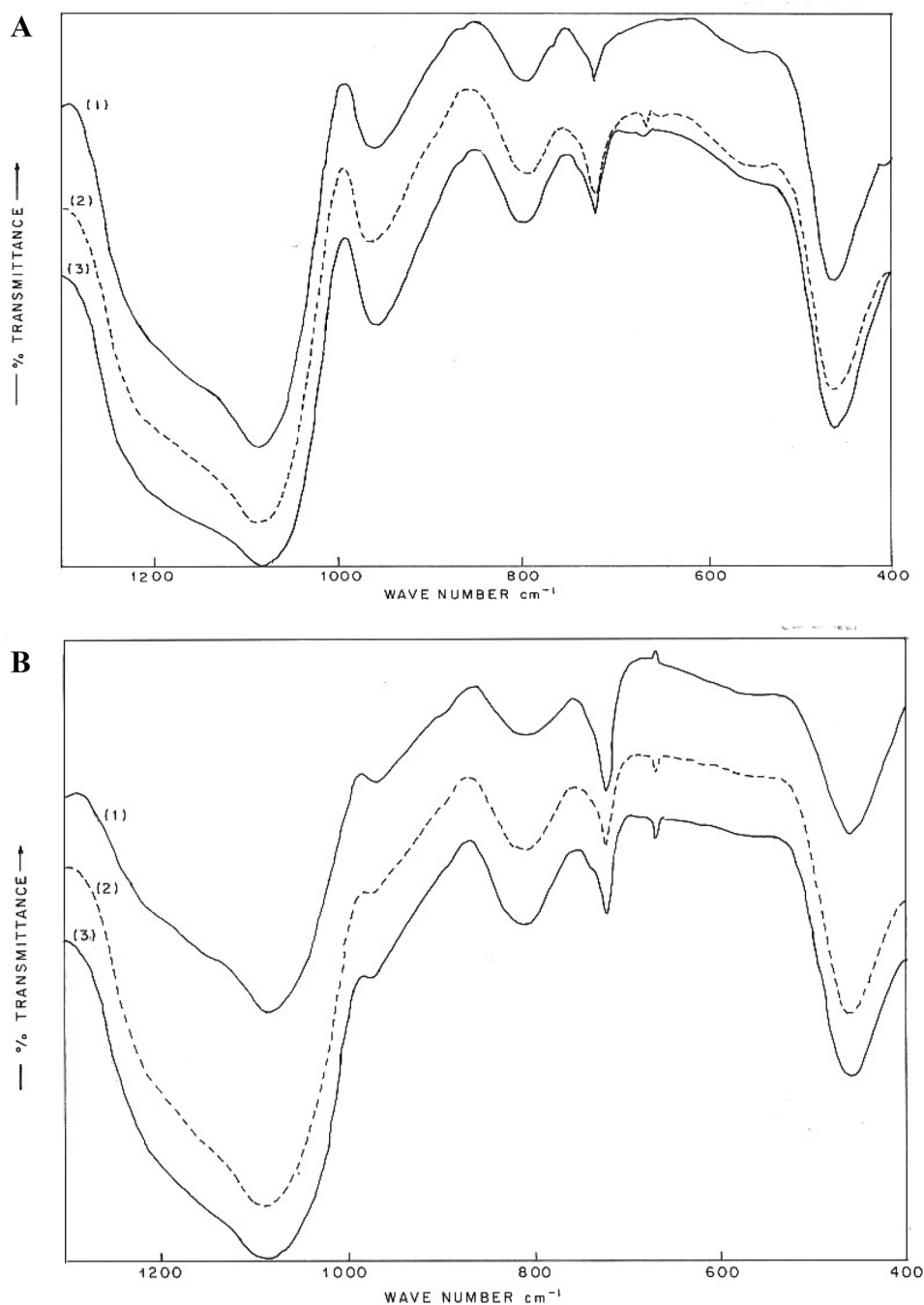
3.1 FTIR spectroscopy

Mesoporous silica materials have been prepared via sol-gel reactions of TEOS in the presence of T, M or C acids as templates. All characteristic absorption bands due to asymmetric stretching mode ($1088\text{--}1084\text{ cm}^{-1}$) with shoulder at $\sim 1200\text{ cm}^{-1}$ and others at 960 cm^{-1} , 800 cm^{-1} , 730 cm^{-1} , 550 cm^{-1} and 450 cm^{-1} assigned to symmetric stretching and deformation mode are observed like other mesoporous silica materials [53]. On comparing the set of spectra A & B in Fig. 1, it has been observed that band intensity at 960 cm^{-1} (due to coupled mode of Si–O stretching and O–H deformation) is lower for calcined samples than for the soxhlet extracted samples. This intensity reduction may be related to dehydroxylation and rearrangement of silica wall during calcination. All the mesoporous silica samples show the absence of strong absorption band at $\sim 1700\text{--}1750\text{ cm}^{-1}$ corresponding to the C=O stretching vibration of hydroxycarboxylic acid indicate that all template molecules are completely removed after washing the silica material (Figure not shown) [53, 54].

3.2 X-ray diffraction

The representative low angle XRD pattern of (A) mesoporous silica SST and (B) corresponding mesoporous carbon SCT are shown in Fig. 2. XRD pattern of mesoporous silica SST, shows a broad diffraction peak (100 reflection) centered at $2\theta = 1.1^\circ$ suggesting short range ordering of mesoporous silica material, which corresponds to d spacing of 8.0 nm. Whereas slight shift in the peak positions (the prominent peak at 100 reflection shifted to higher 2θ value of 1.4° , d-spacing of 7.4 nm) is observed for the corresponding mesoporous carbon material. The XRD pattern of mesoporous carbon in the high angle region ($10\text{--}90^\circ$) showed the absence of peaks characteristic of graphitized carbon which observed at ($2\theta = 26^\circ$ and 44°) assigned to (002) and (10) diffraction of the graphitic framework (Fig. 3). Hence this is highly amorphous carbon with negligible graphitic content which is undetectable by XRD.

Fig. 1 (a): FTIR spectra of soxhlet extracted mesoporous silica materials; (1) SST, (2) SSM and (3) SSC. (b) FTIR spectra of calcined mesoporous silica; (1) CST, (2) CSM and (3) CSC



The XRD pattern of immobilized catalyst Rh-SCT is similar to the parent mesoporous carbon SCT at low angle indicating that the structure of SCT is intact after immobilization of HRhCO(TPPTS)₃ complex (Figure not shown).

3.3 Adsorption studies

N₂ adsorption-desorption isotherms of all the silica/carbon samples exhibit type IV isotherm with type H₂ hysteresis loop which can be attributed to capillary condensation taking

place in the mesoporous silica /carbon samples [33]. The representative tartaric acid templated mesoporous silica's obtained by soxhlet extraction method i.e. SST and calcination method i.e. CST (Figs. 4a and 5a) and their carbon replicas i.e. SCT and CCT respectively (Figs. 4b and 5b) show type IV isotherm with corresponding Barret Joyner Halenda (BJH) pore size distribution plots (insert) determined from the desorption branch of N₂ isotherm. The initial part of type IV isotherm at lower relative pressure ($P/P_0 < 0.4$) is

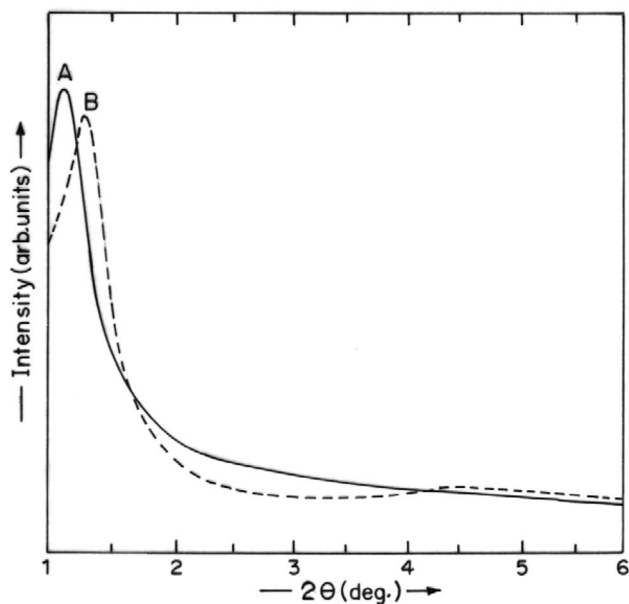


Fig. 2 XRD pattern of (a) mesoporous silica SST and (b) mesoporous carbon replica SCT

mainly attributed to the monolayer multilayer adsorption of mesopores [52].

It is observed that surface area, pore volume and pore diameter of all mesoporous silica samples obtained by soxhlet extraction i.e. SST, SSM and SSC are higher than the respective samples obtained by calcination method i.e. CST, CSM and CSC (Table 1). This behavior may be attributed to the rearrangement of the silica wall due to dehydroxylation and thermal decomposition of corresponding hydroxy carboxylic acid, during slow heating up to 550 °C (Fig. 4). The BET surface area (700 m²/g.) and total pore volume (0.85 cm³/g.) of SST samples are comparable to those of the mesoporous materials prepared by us using surfactants as templates [55].

All mesoporous silica templated carbon samples show greater surface area and pore volume than the respective

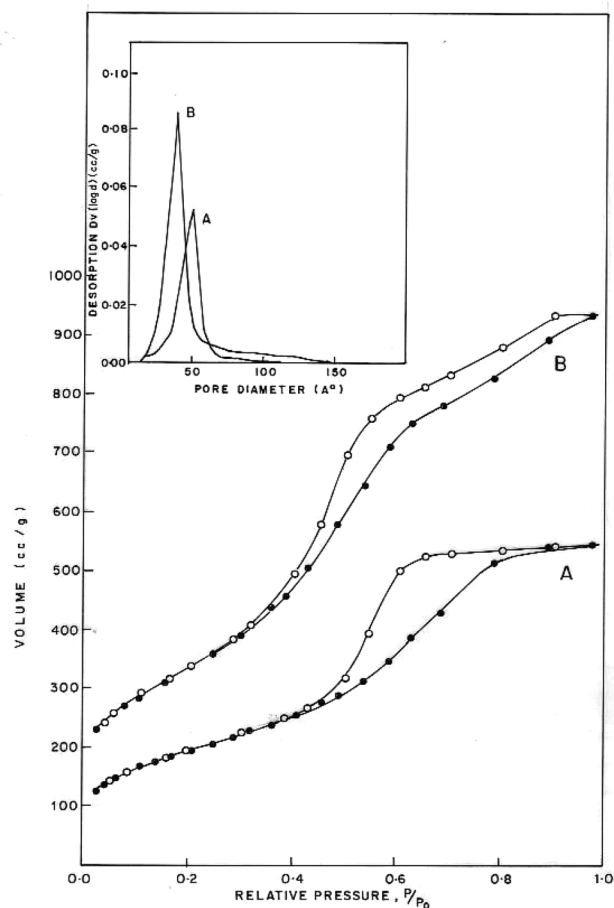
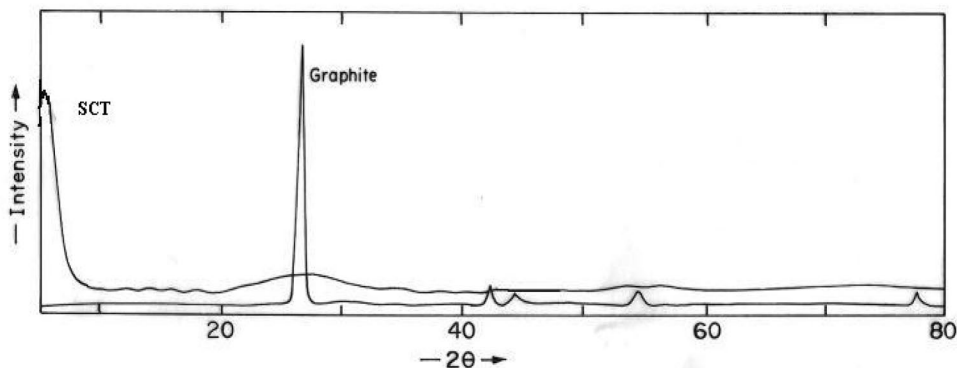


Fig. 4 N₂ adsorption-desorption isotherm and corresponding pore size distribution plots (insert) determined from the desorption branch of N₂ isotherm for the soxhlet extracted mesoporous silica sample (a) SST and its carbon replica (b) SCT

silica templates (Table 1). This observation can be attributed due to microporosity within the carbon walls and the extra porosity due to the incomplete replication process respectively. Mesoporous carbon replica SCT shows higher

Fig. 3 XRD pattern of mesoporous carbon SCT and graphite



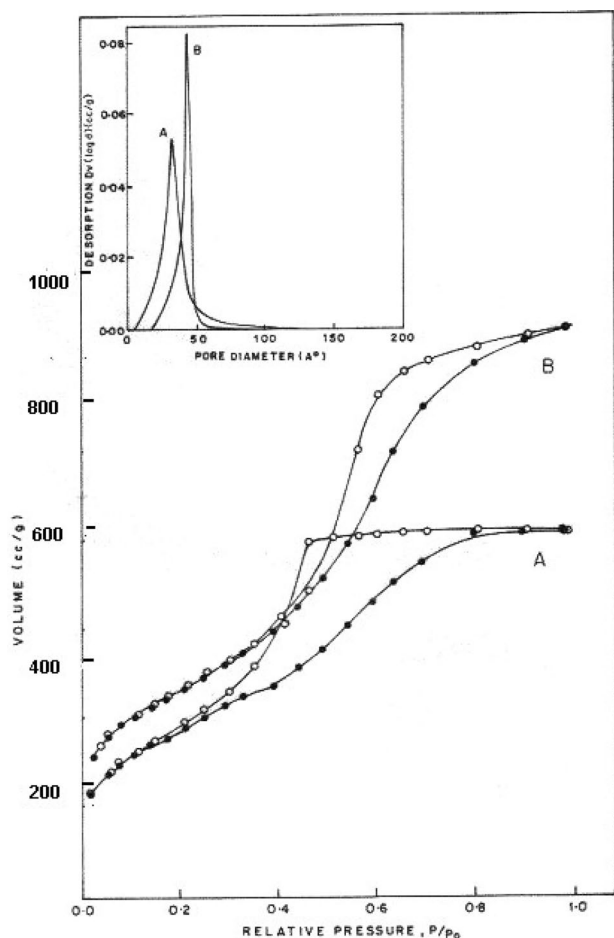


Fig. 5 N_2 adsorption-desorption isotherms and corresponding pore size distribution plots (insert) determined from the desorption branch of N_2 isotherm for the calcined mesoporous silica sample (a) CST and its carbon replica (b) CCT

surface area of $1027 \text{ m}^2/\text{g}$ and pore volume of $1.0 \text{ cm}^3/\text{g}$ than the respective mesoporous silica template SST. The pore diameter of mesoporous carbon material is smaller than the diameter of respective mesoporous silica sample in the case of soxhlet extracted silica samples. Mesoporous silica SST has a pore diameter of 4.8 nm whereas carbon replica SCT shows pore diameter of 3.9 nm . In the case of mesoporous silica samples obtained by calcination method, we observed decrease in the pore diameter as compared to mesoporous silica samples obtained by soxhlet extraction method due to the contraction of pore at the temperature of calcination. Also the pore diameter of calcined sample is smaller than the respective carbon replica. Mesoporous silica sample CST has a pore diameter of 4.0 nm whereas carbon replica shows pore diameter of 4.6 nm . SCT and CCT show the average pore diameter of $\sim 3.9 \text{ nm}$ and 4.6 nm respectively (Fig. 5). This difference in pore diameters may

Table 1 Sorption properties of mesoporous silica templates, corresponding mesostructured carbon replicas and Rh-complex immobilized catalysts

Sample ^a	Pore diameter		$S_{\text{BET}} \text{ m}^2/\text{g}$	Total pore volume cm^3/g	Micropore area m^2/g
	BET nm	BJH nm			
$\text{SiO}_2\text{-gel}^b$	2.0	2.8	325	0.16	285
SST	4.8	4.8	700	0.85	24
SSM	3.7	4.0	879	0.84	22
SSC	5.1	5.0	727	0.93	56
CST	4.4	4.0	664	0.78	15
CSM	4.2	3.8	720	0.83	13
CSC	3.5	3.7	650	0.65	40
SCT	3.5	3.9	1027	1.00	125
SCM	3.9	3.5	1120	0.88	156
SCC	4.6	4.0	1068	1.19	134
CCT	3.6	4.6	1013	0.92	160
CCM	3.5	4.5	981	0.86	96
CCC	4.9	4.5	910	1.00	83
C-1 ^c	1.8	1.7	1142	0.54	1008
Rh-C-1 ^d	1.7	1.7	1124	0.51	994
Rh-SCT ^d	3.2	3.5	390	0.80	33

^aThe first letter of the sample codes abbreviates about the template removing method, S- soxhlet extraction, C- calcination; the second letter denotes as S- mesoporous silica or C- mesoporous carbon; the third letter refers to the template used for building the unit, T- tartaric acid; M- malic acid; C- citric acid

^bControl sample: sol gel SiO_2 prepared without template

^cActivated microporous carbon

^dRh- content is $0.37\% \text{ w/w}$ by ICP analysis

be attributed to respective wall thickness of silica materials i.e. SST $\sim 3.7 \text{ nm}$ and CST $\sim 4.2 \text{ nm}$. In general it is observed that the pore diameters are in the order: SCA $<$ SSA and CCA $>$ CSA. The pore diameters observed for the above-prepared mesoporous carbons are comparable to the carbon materials derived from MCM-48 [21], SBA-15 and MSU-H [56]. From the t-plot analysis with Harkins Jura Equation (Table 1), the measured surface areas and pore volumes in the pure silica powder ($\text{SiO}_2\text{-gel}$) are predominantly contributed by micropores. We observed higher pore diameter of mesoporous carbon than the corresponding silica wall thickness, which may be due to the shrinkage of carbon wall as reported by Jun et al. [21].

Rhodium complex impregnated catalyst Rh-SCT shows decrease in the surface area, pore volume and pore diameter as compared to parent mesoporous carbon SCT as shown in Table 1. This indicates that the pores of SCT are occupied by the metal complex. On the other hand the activated microporous carbon C-1 did not show much change in the surface area after impregnation of metal complex (Table 1). This is due to the microporous nature of C-1 (pore diameter $< 18 \text{ \AA}$)

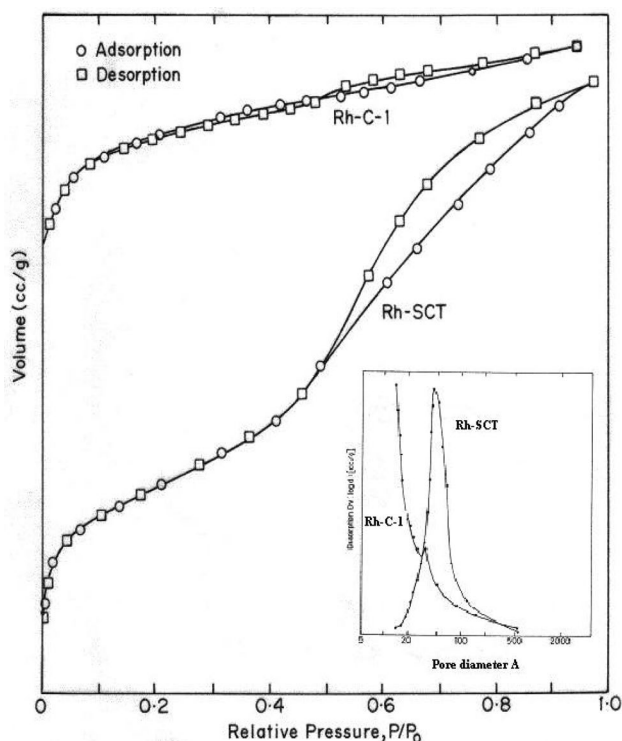
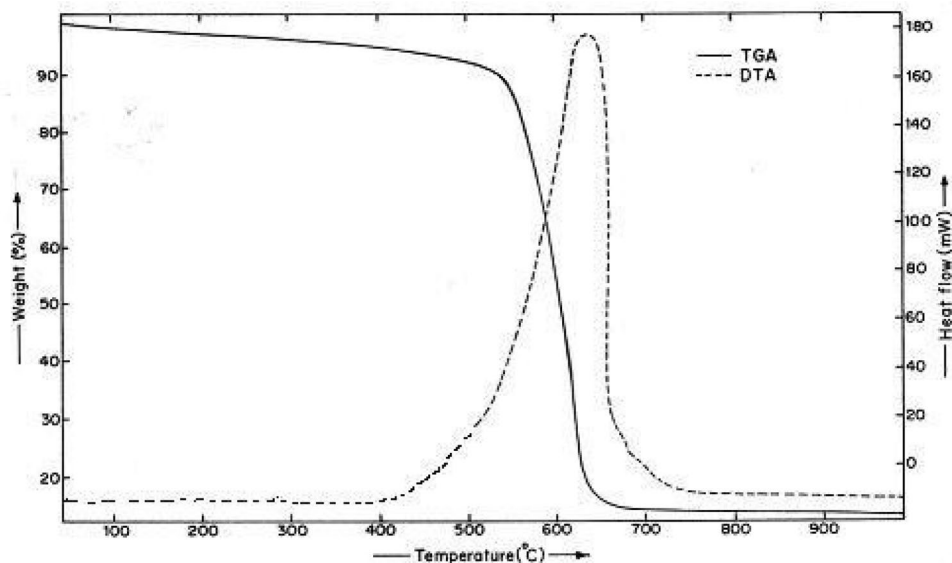


Fig. 6 N_2 adsorption-desorption isotherms and corresponding pore size distribution plots (insert) determined from the desorption branch of N_2 isotherm for Rh-SCT and Rh-C-1

which may not be sufficient to accommodate the bulky metal complex. Figure 6 show the N_2 -sorption isotherms of Rh-SCT and Rh-C-1 with the pore size distribution (inset).

Fig. 7 TGA and DTA curves of mesoporous carbon SCT



^{31}P NMR spectra of Rh-SCT shows shift in the signals as compared to catalyst $HRhCO(TPPTS)_3$ could be a result of interaction of the catalyst with support (Supporting information Fig. S1). This observation was identical to that of previously reported [48].

3.4 Thermal analysis

TG/DTA profile of representative mesoporous carbon SCT is shown in Fig. 7. Thermogravimetric weight change recorded under air shows significant weight loss in narrow temperature range between 550° and 640° ($\sim 98\%$) due to the combustion and decomposition of carbon to CO_2 . This temperature is much lower than that reported for nanotubes and other graphitized carbons which provides confirmation of non-graphitized nature of SCT carbon sample.

3.5 Transmission electron microscopy

TEM images of mesoporous silica material SST and mesoporous carbon replica SCT are shown in Fig. 8a, b respectively. Aggregation of the non-surfactant template molecules could play an important role and the hydrogen bonding between the aggregated templates like folic acid in isotropic water solution [57] and the inorganic precursors in solution and/or during the gelation may direct mesophase formation. These samples show wormhole like channel array together with regions of regular ordering of the pores in parallel arrangements to the channels as seen from TEM images similar to MSU-Si [58], whereas Pang et al. [33] reported the formation of mesoporous silica with wormhole channels only. This may be due to the slow

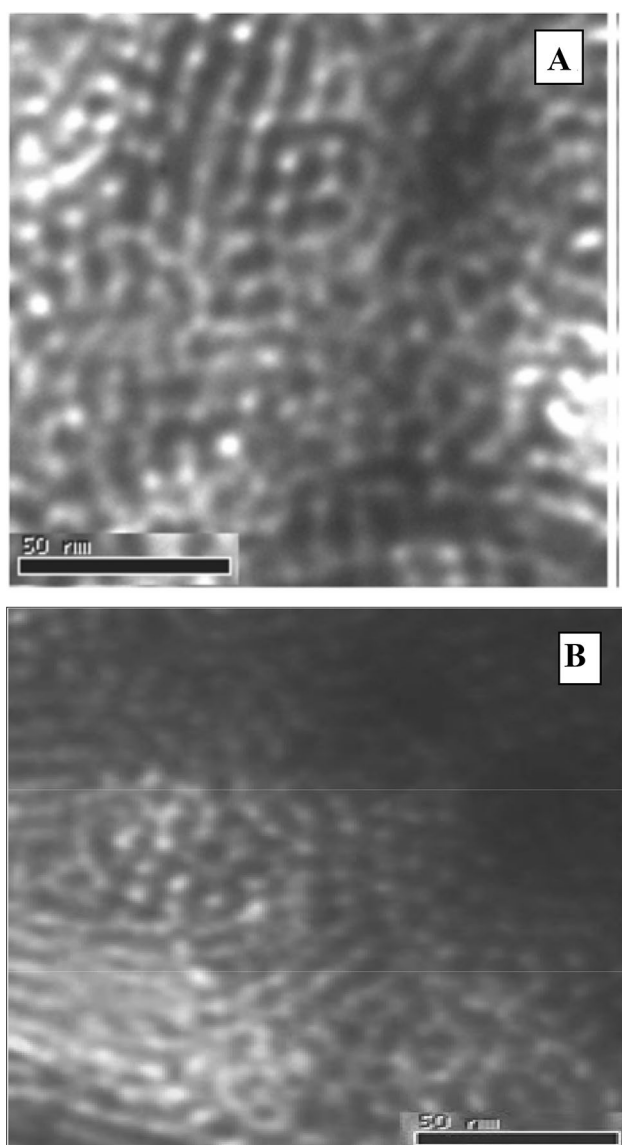


Fig. 8 TEM images of mesoporous silica (a) SST and respective mesoporous carbon replica (b) SCT

hydrolysis of TEOS at room temperature in the presence of templates in the present study.

3.6 Catalytic reactions

Hydroformylation of 1-hexene, 1-octene and 1-decene was carried out using both the catalysts i.e. Rh-C-1 and Rh-SCT at 353 K. We have observed a low n/i aldehyde product ratio in all the reactions. This is due to the formation of internal olefins by isomerization and their subsequent hydroformylation (Table 2).

It was observed that, mesoporous carbon supported Rh-SCT catalyst showed approximately 20–30% higher reaction rates as compared to Rh-C-1 [48, 59]. In addition, this catalyst also gives better activity (TOF) than the literature reported immobilized catalyst for hydroformylation of higher olefins [42, 44, 60–62]. For example for hydroformylation of 1-decene the TOF obtained using Rh-SCT catalyst is 541 h^{-1} , whereas for encapsulated catalyst (TOF = 109 h^{-1}) [44] and for tethered catalyst (TOF = 328 h^{-1}) [42] was obtained under identical reaction conditions. The enhanced activity as compared to Rh-C-1 can be attributed to the large pore diameter (39 \AA) of the support SCT which is sufficient to accommodate the bulky metal complex. This is evident from sorption study which shows a decrease in the surface area after the metal complex is immobilized. Hence interaction of the olefins and diffusion of the product is easier in the case of Rh-SCT.

On the other hand, the activated carbon C-1 with large surface area ($1141 \text{ m}^2/\text{g}$) and a micropore diameter of $\sim 18 \text{ \AA}$ did not show major decrease in the surface area ($>2\%$ decrease) after impregnation of the metal complex i.e. for Rh-C-1. In this case the metal complex primarily occupies the external surface area of the support as the pore size is very small to accommodate the complex. This results in the less dispersed catalyst with a reduced surface area available for the reaction. This lowers the activity of

Table 2 Comparative study of hydroformylation reaction on Rh-C-1 and Rh-SCT catalysts

Sr no	Catalyst	Olefin	% Conversion	% aldehyde. Selectivity	% Final Isomerisation	n/i	TOF/h.	Time, h
1	Rh-C-1	1-hexene	100	91.4	8.6	1.05	629	4.33
2	Rh-SCT	1-hexene	100	97.1	2.9	0.79	873	3.50
1	Rh-C-1	1-octene	98.6	95.3	4.7	0.93	549	5.22
2	Rh-SCT	1-octene	99.3	98.3	1.7	0.74	673	4.50
1	Rh-C-1	1-decene	97.2	99.3	0.74	0.74	473	6.07
2	Rh-SCT	1-decene	99.4	96.9	3.1	0.65	541	5.42

Reaction conditions: Temperature 353 K, Stirring speed 1000 rpm, $p_{\text{CO}+\text{H}_2}$ (1:1) 4.14 MPa, olefin: 0.391 kmol/m^3 Catalyst: 0.100 g (Rh content 0.37% w/w), Total charge $2.7 \times 10^{-5} \text{ m}^3$, solvent: toluene

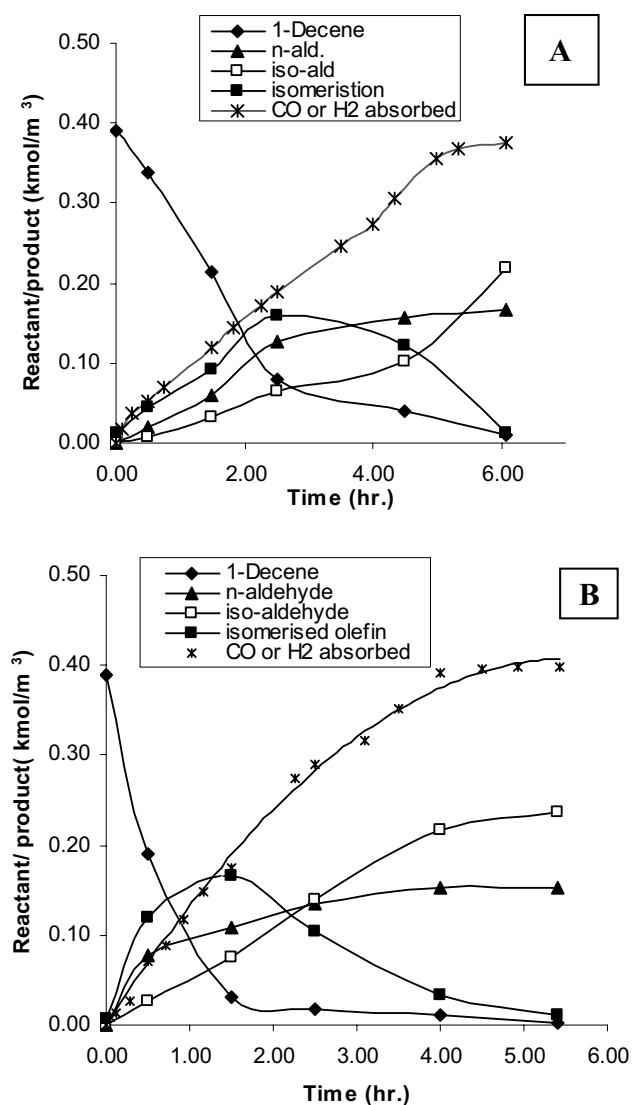


Fig. 9 C.T. Profile for hydroformylation of 1-decene using (a) Rh-C-1 and (b) Rh-SCT Catalyst. Reaction conditions: Temperature 353 K, Stirring speed 1000 rpm, $p_{\text{CO} + \text{H}_2}$ (1:1) 4.14 MPa, 1-decene: 0.391 kmol/m^3 Catalyst: 0.100 g (Rh content 0.37% w/w), Total charge $2.7 \times 10^{-5} \text{ m}^3$, solvent: toluene

the catalyst as compared to mesoporous carbon SCT supported catalyst Rh-SCT.

Figure 9a, b shows a comparison between concentration time profile for hydroformylation of 1-decene using Rh-C-1 and Rh-SCT catalyst respectively. The product profiles were the same. In both the cases it was observed that syngas ($\text{CO} + \text{H}_2$) and 1-decene consumed were consistent with the amount of aldehyde formed. The time required for complete conversion of 1-decene to the product aldehyde is lesser for Rh-SCT catalyst compared to Rh-C-1 catalyst

4 Conclusion

Mesoporous silica material having wormhole channels along with some regions of regularly ordered channel arrangement was prepared at room temperature using low-cost non-surfactant templating agents. This silica material with three dimensional interconnected channel arrangements was used as a template to prepare mesoporous carbon material with surface area $\sim 1100 \text{ m}^2/\text{g}$ and pore diameter in the range of 4–5 nm. Mesoporous carbon supported ossified catalyst was obtained by precipitating barium salt of $\text{HRh}(\text{CO})(\text{TPPTS})_3$ complex. The catalyst was found to be highly stable and physically adsorbed onto the support. The catalyst shows better catalytic activity (TOF) and comparable aldehyde selectivity over the catalyst formed using conventional activated carbon support for hydroformylation of higher olefins.

Acknowledgements Authors would like to acknowledge the partial financial support by CSIR network project (CMM0005): Catalysis and Catalysts.

References

1. C.R. Bansal, J.B. Donnet, F. Stoeckli, *Active Carbon* (Marcel Dekker, New York, 1998)
2. H.C. Foley, *J. Microporous Mater.* **4**(6), 407–433 (1995)
3. V.M. Ortiz-Martínez, L. Gómez-Coma, A. Ortiz, I. Ortiz, *Rev. Chem. Eng.* (2019). <https://doi.org/10.1515/revce-2018-0056>
4. M.R. Benzigar, S.N. Talapaneni, S. Joseph, K. Ramadass, G. Singh, J. Scaranto, U. Ravon, K. Al-Bahilyc, A. Vinu, *Chem. Soc. Rev.* **47**, 2680–2721 (2018)
5. T.Y. Ma, L. Liu, Z.Y. Yuan, *Chem. Soc. Rev.* **42**, 3977–4003 (2013)
6. C. Liang, Z. Li, .S. Dai, *Angew. Chem. Int. Ed.* **47**, 3696–3717 (2008)
7. T. Kyotani, *Carbon* **38**(2), 269–286 (2000)
8. J.W. Patrick, *Porosity in Carbon: Characterization and Applications* (Edward Arnold, London, 1995)
9. M. Oschatz, S. Thieme, L. Borchardt, M.R. Lohe, T. Biemelt, J. Bruckner, H. Althues, S. Kaskel, *Chem. Commun.* **49**, 5832–5834 (2013)
10. K. Zhang, S. Tao, X. Xu, H. Meng, Y. Lu, C. LiJan, *Ind. Eng. Chem. Res.* **57**(18), 6180–6188 (2018)
11. H. Marsh, *Introduction to Carbon Science*, 1st edn. (Butterworths, London, 1989)
12. S. Han, K. Sohn, T. Hyeon, *Chem. Mater.* **12**(11), 3337–3341 (2000)
13. S. Yoon, J. Lee, T. Hyeon, S.M. Oha, *J. Electrochem. Soc.* **147**, 2507–2512 (2000)
14. J.S. Beck, J.C. Vartuli, W.J. Roth, M.E. Leonowicz, C.T. Kresge, K.D. Schmidt, C.T.-W. Chu, D.H. Olson, E.W. Sheppard, S.B. McCullen, J.B. Higgins, J.L. Schlenker, *J. Am. Chem. Soc.* **114**(27), 10834–10843 (1992)
15. P.T. Tanev, T.J. Pinnavaia, *Science* **267**(5199), 865–867 (1995)
16. A. Monnier, F. Schuth, Q. Huo, D. Kumar, D. Margolese, R.S. Maxwell, G.D. Stucky, M. Krishnamurty, P. Petroff, A. Firouzi, M. Janicke, B.F. Chmelka, *Science* **261**(5126), 1299–1303 (1993)

17. Q. Huo, D.I. Margilese, U. Ciesla, P. Feng, T.E. Gier, P. Sieger, R. Leon, P.M. Petroff, F. Schuth, G.D. Stucky, *Nature* **368**, 317–321 (1994)
18. J.A. Cecilia, R.M. Tost, M.R. Millan, *Int. J. Mol. Sci.* **20**, 3213–3016 (2019)
19. S. Kumar, M.M. Malik, R. Purohit, *Mater. Today Proc.* **4**, 350–357 (2017)
20. R. Ryoo, S.H. Joo, S. Jun, *J. Phys. Chem. B* **103**(37), 7743–7746 (1999)
21. S. Jun, S.H. Joo, R. Ryoo, M. Kruk, M. Jaroniec, Z. Liu, T. Ohsuna, O. Terasaki, *J. Am. Chem. Soc.* **122**(43), 10712–10713 (2000)
22. T.-W. Kim, R. Ryoo, K.P. Gierszal, M. Jaroniec, L.A. Solovyov, Y. Sakamoto, O. Terasaki, *J. Mater. Chem.* **15**, 1560–1571 (2005)
23. J. Lee, S. Yoon, S.M. Oh, C.H. Shin, T. Hyeon, *Adv. Mater.* **12**(5), 359–362 (2000)
24. W.W. Lukens, G.D. Stucky, *Chem. Mater.* **14**(4), 1665–1670 (2002)
25. M. Sevilla, S. Alvarez, A.B. Fuertes, *Microporous Mesoporous Mater.* **74**(1–3), 49–58 (2004)
26. M. Kim, K. Sohn, J. Kim, T. Hyeon, *Chem. Commun.* **5**, 652–653 (2003)
27. S. Han, M. Kim, T. Hyeon, *Carbon* **41**(8), 1525–1532 (2003)
28. N.K. Raman, M.T. Anderson, C.J. Brinker, *Chem. Mater.* **8**(8), 1682–1701 (1996)
29. C.T. Kresge, M.E. Leonowicz, W.J. Roth, J.C. Vertuli, J.S. Beck, *Nature* **359**, 710–712 (1992)
30. C. Gerardin, J. Reboul, M. Bonne, Benedicte Lebeau, *Chem. Soc. Rev.* **42**, 4217–4255 (2013)
31. S.A. Bagshaw, E. Prouzet, T.J. Pinnavaia, *Science* **269**(5228), 1242–1244 (1995)
32. Y. Wei, D.T. Ding, W.H. Shih, X. Liu, S.Z.D. Cheng, Q. Fu, *Adv. Mater.* **3**(4), 313–316 (1998)
33. J.B. Pang, K.Y. Qiu, Y. Wei, *J. Non-Cryst. Solids* **283**(1–3), 101–108 (2001)
34. J.B. Pang, K.Y. Qiu, Y. Wei, *Chem. Mater.* **13**, 2361–2365 (2001)
35. J.Y. Zheng, J.B. Pang, K.Y. Qiu, Y. Wei, *J. Sol-Gel Sci. Technol.* **24**, 81–88 (2002)
36. H. Misran, R. Singh, M. Ambar, *Yarmo Microporous Mesoporous Mater* **112**, 243–253 (2008)
37. Z. Chen, B. Peng, J.Q. Xu, X.C. Xiang, D.F. Ren, T.Q. Yang, S.Y. Ma, K. Zhang, Q.M. Chen, *Nanoscale* **12**, 3657–3662 (2020)
38. P. W. N. M. van Leeuwen, C. Claver (eds.), *Rhodium Catalyzed Hydroformylation* (Kluwer Academic Publishers, London, 2002)
39. P. Barbaro, F. Liguori (eds.), *Heterogenized Homogeneous Catalysts for Fine Chemicals Production* (Springer, Dordrecht, 2010)
40. R.L. Augustine, S.K. Tanielyan, N. Mahata, Y. Gao, A. Zsigmond, H. Yang, *Appl. Catal. A Gen.* **256**(1–2), 69–76 (2003)
41. R.L. Augustine, P. Goel, N. Mahata, C. Reyes, S.K. Tanielyan, *J. Mol. Catal. A Chem.* **216**(2), 189–197 (2004)
42. K. MuKhopadhyay, R.V. Chaudhari, *J. Catal.* **213**(1), 73–77 (2003)
43. S. Sadjadi (ed.), *Encapsulated Catalysts* (Academic Press, London, 2017)
44. K. Mukhopadhyay, A.B. Mandale, R.V. Chaudhari, *Chem. Mater.* **15**(9), 1766–1777 (2003)
45. A. Riisager, R. Fehrmann, M. Haumann, P. Wasserscheid, *Eur. J. Inorg. Chem.* **2006**(4), 695–706 (2006)
46. J.P. Arhancet, M.E. Davis, J.S. Merola, B.E. Hanson, *Nature* **339**, 454–455 (1989)
47. B.R. Sarkar, R.V. Chaudhari, *J. Catal.* **242**, 231–238 (2006)
48. N.S. Pagar, R.M. Deshpande, R.V. Chaudhari, *Catal. Lett.* **110**(1–2), 129–133 (2006)
49. R.V. Chaudhari, A.N. Mahajan, *US Patent* 7,026,266 (2006)
50. B.R. Sarkar, R.V. Chaudhari, *Platin. Met. Rev.* **54**(2), 73–80 (2010)
51. J.P. Arhancet, M.E. Davis, J.S. Merola, B.E. Hanson, *J. Catal.* **121**(2), 327–339 (1990)
52. A.A. Zahidov, R.H. Banghman, Z. Jgbal, C. Lui, I. Khayrullin, S.O. Dantas, J. Marti, V.G. Rachenko, *Science* **282**(5390), 897–901 (1998)
53. P. Karandikar, M. Agashe, K. Vijayamohan, A.J. Chandwadkar, *Appl. Catal. A Gen.* **257**, 133 (2004)
54. P. Karandikar, K.R. Patil, A. Mitra, B. Kakadec, A.J. Chandwadkar, *Microporous Mesoporous Mater.* **98**(1–3), 189–199 (2007)
55. K. Chaudhari, T.K. Das, P.R. Rajmohan, K. Lazar, S. Sivasanker, A.J. Chandwadkar, *J. Catal.* **183**(2), 281–291 (1999)
56. S.S. Kim, T.J. Pinnavaia, *Chem. Commun.* **23**, 2418–2419 (2001)
57. G. Gottarelli, E. Mezzina, G.P. Spada, F. Carsughi, G. Di Nicola, P. Mariani, A. Sabatucci, S. Bonazzi, *Helv. Chem. Acta* **79**(1), 220–234 (1996)
58. A. Infantes-Molina, J. Merida-Robles, P. Maireles-Torres, E. Finocchio, G. Busca, E. Rodriguez-Castellon, J.L.G. Fierro, A. Jimenez-Lopez, *Microporous Mesoporous Mater.* **75**(1–2), 23–32 (2004)
59. N.S. Pagar, R.M. Deshpande, *Int. J. Chem. Kinet.* **51**, 112–122 (2019)
60. M. Nowotny, T. Maschmeyer, B.F.G. Johnson, P. Lahuerta, J.M. Thomas, J.E. Davies, *Angew. Chem. Int. Ed.* **40**(50), 955–958 (2001)
61. S.K. Sharma, P.A. Parikh, R.V. Jasra, *J. Mol. Catal. A Chem.* **316**, 153–162 (2010)
62. X. Jia, Z. Liang, J. Chen, J. Lv, K. Zhang, M. Gao, L. Zong, C. Xie *Org. Lett.* **21**(7), 2147–2150 (2019)

Publisher's Note Springer Nature remains neutral with regard to jurisdictional claims in published maps and institutional affiliations.